MODELING DEPOSITION FROM DENSE PYROCLASTIC DENSITY CURRENTS ON VENUS. I. Ganesh[1] (indujaa@email.arizona.edu), L. McGuire[2] and L. M. Carter[1], [1]Lunar and Planetary Laboratory, University of Arizona, Tucson AZ 85721, [2]Department of Geosciences, University of Arizona, Tucson AZ 85721.

Introduction: Radar-bright summit features associated with some volcanic centers on Venus have been proposed to be deposited from pyroclastic density currents (PDCs) [1,2]. These deposits have diffuse margins that expose underlying lava flows, high radar backscatter in Magellan SAR, and lack flow structures in the deposit interior, all of which are consistent with a rough-textured mantling layer of clastic debris [1]. The extent of continuous bright material from the summit to the deposit terminus ranges from 40 – 120 km. While such long runout PDC eruptions are not observed in the present day, older (>1800 yr. BP) PDC deposits extending for more than 100 km from the source are found at many places on Earth [3-7]. In this study, we model PDC propagation under Venus conditions to constrain the physical properties of PDCs required to emplace long runout deposits.

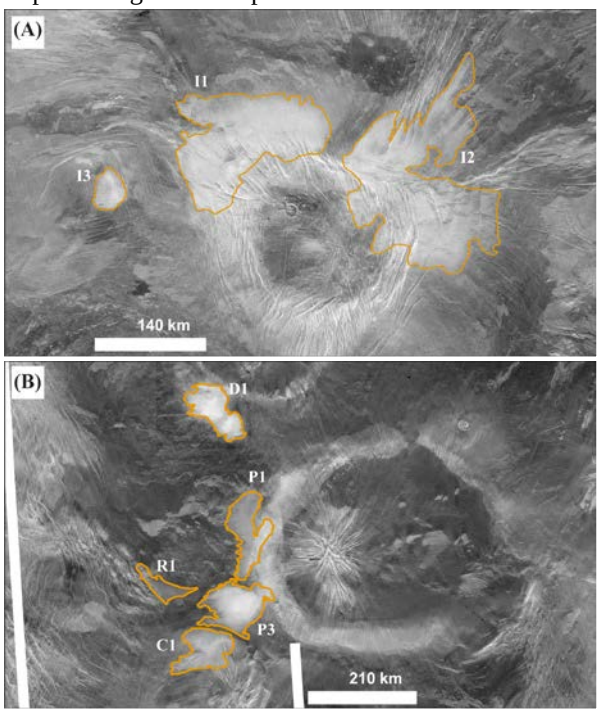

Fig. 1: Magellan SAR image of (A) Irnini Mons and (B) Pavlova Corona. Radar-bright diffuse deposits have been mapped in yellow based on [1].

Study sites: We initially focus on the deposits at two different sites in Eistla Regio – Irnini Mons (Fig. 1A) and Pavlova Corona (Fig. 1B) Irnini Mons (14.3°N, 15.65°E) is a volcano-tectonic construct with two radar-bright, diffuse deposits marked I1 and I2 at the northern summit (Fig. 1A). These deposits appear to originate at the corona margins and extend down slopes of ~1.2° up to distances of ~70 km. Similar diffuse deposits have been noted in the western and southwestern flanks of Pavlova Corona (14.5°N, 40°E) and Didilia Corona (18°N, 37.3°E) (Fig. 1B). These deposits extend up to ~100 km from the corona margins down shallower slopes (~0.3°). Due to model run time and stereo-DEM [8] coverage constraints, we have so far limited our focus to one proposed PDC deposit at each of these sites, I2 and P1, for the present study. Runout distances for P1 range from 40 – 60 km while I2 has a longer extent with a maximum runout of ~110 km.

Pyroclastic flow model: The pyroclastic current is treated as a two-component granular flow with ~30% volume fraction of solids (ash, pumice and lithics) supported by excess pore fluid pressure in a laminar Newtonian fluid [9]. We solve depth averaged shallow water equations in 2D to determine the thickness and velocity of the current at each point in time and space. The current is primarily driven by gravity and the motion of the current is opposed by friction and viscous resistance. A shear-rate dependent variable basal friction model is used to determine the basal friction as the flow evolves [10]. Stereo DEMs generated from Magellan left-look data have been used as input topography for all simulations [8]. A 1st order Godunov scheme with an HLLC Riemann solver is used to calculate the flux across cell interfaces and the source terms are solved separately using an explicit Euler method. This approach of modeling PDCs as grain flows has been shown to be effective for pyroclastic flows on Earth [11, 12].

Model limitations. This simplified 2D model assumes initial conditions arising from the instantaneous collapse of constant volume columns. This has implications for modeling both the flow thickness and the velocity. The flow dynamics immediately following instantaneous collapse is not captured effectively by the shallow water equations. However, the model is well suited for describing the flow as it evolves away from the initial conditions towards flow depths that are much smaller compared to the flow's areal extent. Instantaneous column collapse imparts high initial velocity that might drive the flow to turbulent regimes. But once past this initial phase, the flow slows down to velocities required for non-turbulent propagation captured by the model. Additionally, the granular flow model approach only simulates dense flows in which the effects due to entrainment of the Venusian atmosphere are negligible.

Initial conditions. We use a bulk flow viscosity of 10^{-1} Pas, and a bulk flow density corresponding to a

dielectric permittivity ε' = 3. Starting velocity of 100 ms^{-1} and initial interstitial fluid pressure to basal stress ratio of 0.98 are used. Table 1 shows the initial parameter values used for both deposits. We chose 10 locations with good stereo topography along the corona margins to represent multiple eruption centers that were the likely source of PDCs (solid white circles in Fig. 2). Results from the simulations for parameters specified in Table 1 are discussed below.

Deposit name	I2	P1
Total volume (km^3)	125	38
Initial velocity (ms^{-1})	100	100
Initial pore fluid pressure	0.98	0.98

Table 1: Parameter values used in the simulation

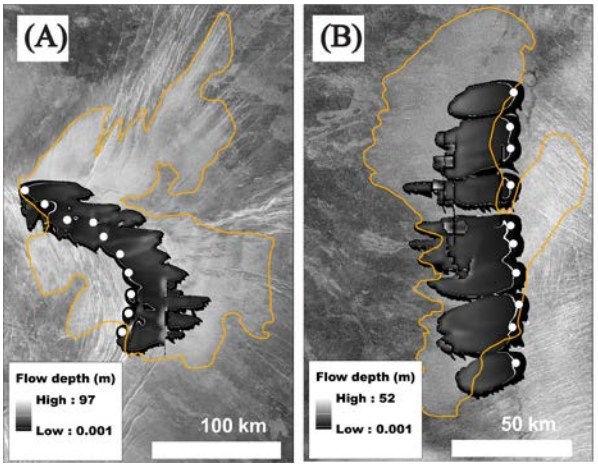

Fig. 2: Modeled deposit thickness for (A) I2 at Irnini Mons and (B) P1 at Pavlova Corona using parameters in Table 1. Solid white circles show the location of initial source vents along the corona margins. Downslope direction is towards East for I2 and towards West for P1. Vertical artifacts in (A) occur at sites where there are gaps in stereo DEM.

Results and Discussion: The location of the initial columns and the final runout of the PDCs are shown for both I2 (Fig. 2A) and P1 (Fig. 2B). For I2, the modeled deposit thickness ranges from a few meters close to the source to < 50 km on the slopes. Thicker deposits (40 – 97 m) are predicted to infill a graben extending around the eastern margin. Similar infilling is also predicted in lower relief radial fractures. The modeled flow comes to rest at a maximum distance of ~60 km from the source, which is only ~0.5 times the observed deposit extent. In the case of P1, the modeled deposit thickness has a high of ~50 m. Similar to I2, the thicker deposits are predicted to occur towards the terminus. The western flank of Pavlova does not have low relief features, and this is reflected in the model where no localized thickening of deposits is predicted. The modeled runout is typically <45 km with most flows having ceased propagation around 30 km. The modeled flows match the observed runout only in places where the runout is lowest (~40 km).

Most of the predicted runouts are 0.4 – 0.65 times measured runout lengths. Longer runouts can be generated by the model using larger deposit volumes, higher initial velocities, and higher ratio of pore fluid pressure to basal stress in the model parameters. The pore fluid pressure to basal stress ratio used here is already quite high (0.98). Ideally, it is possible for PDCs to have a maximum velocity equal to the speed of sound (~400 ms^{-1} on Venus). However, higher velocity flows begin to develop turbulence which limits the distances to which larger clasts can be transported. Large volume flows will be thicker, thereby making the diffusion of the interstitial fluid pressure slower. The sustained high pore fluid pressure helps in mobilizing flows for longer distances. But it is important to note that large flow thicknesses also induce turbulence. It has been proposed that semi-fluidized PDCs more than a few meters thick moving faster than 15-60 ms^{-1} will develop turbulence [13]. If the Venus deposits have a PDC-origin, it is likely that they were deposited from a steady current generated from sustained fountaining or boiling-over which would ensure continued supply of volume at low velocities resulting from shorter collapse heights.

Future work: The next step is to explore the parameter space more thoroughly for the PDCs shown in Fig. 1 and extend the model simulations for other proposed PDCs [1]. We also intend to explore turbulence driven PDC transport that has been suggested to the mechanism of emplacement for large ignimbrite sheets such as Taupo ignimbrites [14].

Acknowledgments: This study was supported by a FINESST award to I. Ganesh and partly by an SSW grant to L. M. Carter. Magellan SAR images were processed using USGS Astrogeology Science Center's Map-A-Planet 2 (MAP2).

References: [1] Campbell B. A. et al. (2017) *JGR 122*, 1580–1596. [2] Ghail R. C. and Wilson. L. (2015) *Geological Soc. Lond. Spl. Pub. 401*. [3] Roche, O. et al. (2016) *Nat. Comm.* 7:10890. [4] Wilson, C. J. N. et al. (1995) *Nature 378*, 605–607. [5] Streck M. J. and Grunder A. L. (1995) *Bull Volcanol 57*, 151-169. [6] Henry C. D. et al. (2012) *Geosphere 8*, 1-27. [7] Branney, M. J. and Kokelaar, P. (2002) *Geological Soc. Lond. Mem.* 27. [8] Herrick, R. R. et al. (2012) *EOS Trans. AGU 93*, 125-126. [9] Iverson R. M. and Denlinger R. P. (2001) *JGR, 106*, 537-552. [10] Jop P. et al. (2006) *Nature, 441, 727-730*. [11] Patra A. K. et al. (2005) *JVGR 139*, 1–22. [12] Sheridan M. F. et al. (2005) *JVGR 139*, 89–102. [13] Sparks R. J. (1976) *Sedimentology 23*, 147-188. [14] Bursik M. I. and Woods A. W. (1996) *Bull Volcanol 58*, 175-193.